International Immunopharmacology 24 (2015) 400–407

Contents lists available at ScienceDirect

International Immunopharmacology

journal homepage: www.elsevier.com/locate/intimp

Lipoxin A_4 attenuates endothelial dysfunction during experimental cerebral malaria

Mariana C. Souza [a,b,1], Tatiana A. Pádua [a,b,1], Natália D. Torres [a,b], Maria Fernanda Souza Costa [a,b], André P. Candéa [a,b], Thadeu Maramaldo [a,b], Leonardo Noboru Seito [a], Carmen Penido [a,b], Vanessa Estato [c], Barbara Antunes [c], Leandro Silva [d], Ana Acácia Pinheiro [d], Celso Caruso-Neves [d], Eduardo Tibiriçá [c], Leonardo Carvalho [e], Maria G. Henriques [a,b,*]

[a] Laboratory of Applied Pharmacology, Farmanguinhos, Oswaldo Cruz Foundation, Rio de Janeiro, RJ, Brazil
[b] National Institute for Science and Technology on Innovation on Neglected Diseases (INCT/IDN), Center for Technological Development in Health (CDTS), Oswaldo Cruz Foundation (Fiocruz), Rio de Janeiro, RJ, Brazil
[c] Laboratory of Cardiovascular Investigation, Oswaldo Cruz Institute, Oswaldo Cruz Foundation, Rio de Janeiro, RJ, Brazil
[d] Institute of Biophysics Carlos Chagas Filho, Federal University of Rio de Janeiro, Rio de Janeiro, RJ, Brazil
[e] Laboratory of Malaria Research, Instituto Oswaldo Cruz, Oswaldo Cruz Foundation, Rio de Janeiro, RJ, Brazil

ARTICLE INFO

Article history:
Received 6 November 2014
Received in revised form 23 December 2014
Accepted 24 December 2014
Available online 7 January 2015

Keywords:
Endothelial dysfunction
Lipoxin
Malaria
Brain–blood barrier breakdown

ABSTRACT

A breakdown of the brain–blood barrier (BBB) due to endothelial dysfunction is a primary feature of cerebral malaria (CM). Lipoxins (LX) are specialized pro-resolving mediators that attenuate endothelial dysfunction in different vascular beds. It has already been shown that LXA_4 prolonged *Plasmodium berghei*-infected mice survival by a mechanism that depends on inhibiting IL-12 production and $CD8^+IFN\text{-}\gamma^+$ T cells in brain tissue; however, the effects of this treatment on endothelial dysfunction induced during experimental cerebral malaria (ECM) remains to be elucidated. Herein, we investigate the role of LXA_4 on endothelial dysfunction during ECM. The treatment of *P. berghei*-infected mice with LXA_4 prevented BBB breakdown and ameliorated behavioral symptoms but did not modulate TNF-α production. In addition, microcirculation analysis showed that treatment with LXA_4 significantly increased functional capillary density in brains of *P. berghei*-infected C57BL/6 mice. Furthermore, histological analyses of brain sections demonstrated that exogenous LXA_4 reduced capillary congestion that was accompanied by reduced ICAM-1 expression in the brain tissue. In agreement, LXA_4 treatment of endothelial cells stimulated by *Plasmodium berghei* (*Pb*)- or *Plasmodium falciparum* (*Pf*)-parasitized red blood cells (RBCs) inhibited ICAM-1 expression. Additionally, LXA_4 treatment restored the expression of HO-1 that is reduced during ECM. As well, LXA_4 treatment inhibits *Pb*RBC and *Pf*RBC adhesion to endothelial cells that was reversed by the use of an HO-1 inhibitor (ZnPPIX). Our results demonstrate for the first time that LXA_4 ameliorates endothelial dysfunction during ECM by modulating ICAM-1 and HO-1 expression in brain tissue.

1. Introduction

Malaria is the most widespread parasitic disease, and despite the many efforts made to eradicate malaria, it still accounts for 1 million deaths per year [1]. Death by cerebral malaria is closely associated with the adhesion of parasitized erythrocytes to brain vasculature and breakdown of the blood–brain barrier (BBB) [2,3]. In fact, it has been widely demonstrated that murine experimental cerebral malaria (ECM)-induced endothelial dysfunction depends on the adhesion of parasitized erythrocytes to cerebral microvasculature [4–6]; the production of inflammatory mediators, such as TNF-α, as well as increased expression of adhesion molecules on endothelial cells [7,8]. Recent advances concerning malaria treatment have suggested that an adjuvant therapy targeting endothelial activation improves patient outcome [9–11]. Indeed, prevention of BBB disruption has been shown to diminish ECM [3], which can be achieved *via* pharmacological induction of the stress-responsive protein heme oxigenase-1 (HO-1) and exposure to carbon monoxide, the end-product of HO-1 activity [12].

Lipoxins (LX) are products of arachidonic acid metabolism and are produced through sequential lipoxygenase activity following cell–cell

Abbreviations: AI, adhesion index; BBB, brain–blood barrier; BOC-2, N-Boc-Phe-Leu-Phe-Leu-Phe; CFSE, carboxyfluorescein succinimidyl ester; CM, cerebral malaria; ECM, experimental cerebral malaria; ELISA, enzyme linked immuno sorbent assay; HO, heme oxygenase; ICAM, intercellular adhesion molecule; LX, lipoxin; NO, nitric oxide; *Pb*, *Plasmodium berghei*; *Pf*, *Plasmodium falciparum*; RBC, red blood cell; TNF, tumor necrosis factor; ZnPPIX, zinc protoporphyrin IX.

* Corresponding author at: Laboratory of Applied Pharmacology, Farmanguinhos, Oswaldo Cruz Foundation, Rio de Janeiro, RJ, Brazil.
E-mail address: gracahenriques@fiocruz.br (M.G. Henriques).

[1] These authors equally contributed to this work.

http://dx.doi.org/10.1016/j.intimp.2014.12.033
1567-5769/

interactions in the inflammatory milieu (reviewed by [13]). The interaction of LXA_4 and its receptor, ALX has an anti-inflammatory and pro-resolving activity in several inflammatory models such as allergic airway inflammation [14], autoimmune diseases [15] and inflammatory diseases triggered by bacterial infection [16]. The effect of LXA_4 on endothelial cells includes the stimulation of cytoprotective pathways [17–20]. It has been widely reported that LXA_4 upregulates the expression of heme-oxygenase 1 (HO-1), a stress-responsive enzyme with cytoprotective activities [21]. In fact, the stimulation of HO-1 expression by LXA_4 in endothelial cells is responsible for the inhibition of cellular activation, including decreased expression of adhesion molecules [22].

Recently, Shryock and colleagues [23] demonstrated that, during severe malaria, treatment with LX epimers (15-epi-LXA_4) prolonged survival by a mechanism that depends on inhibiting IL-12 production and $CD8^+IFN\text{-}\gamma^+$ T cell accumulation in brain tissue. However, the effects of this treatment on endothelial dysfunction that is triggered during ECM remain to be elucidated. In the present study, we provide evidence that LXA_4 exerts a protective effect on brain's endothelial cells by beneficially impacting cerebral edema formation and microcirculation. The underlying mechanisms are shown to include the prevention of capillary rarefaction and anti-adhesive/anti-inflammatory effects on endothelial cells.

2. Materials and methods

2.1. Ethics statement

This work was carried out in strict accordance with the recommendations in the Guide for the Care and Use of Laboratory Animals of the National Institutes of Health. The protocol was approved by the Committee on Ethical Use of Laboratory Animals of the Oswaldo Cruz Foundation (permit number L052/12).

2.2. Animal preparation and experimental protocol

Male C57BL/6 mice (5–6 weeks old) were provided by the Oswaldo Cruz Foundation breeding unit (Rio de Janeiro, Brazil) and caged with free access to food and fresh water at the Farmanguinhos experimental facility, with a room temperature ranging from 22 to 24 °C in a 12-hour light/dark cycle. The animals were randomly assigned to three groups: uninfected, *P. berghei*-infected and LXA_4-treated *P. berghei*-infected mice. *P. berghei* ANKA GFPcon 259cl2 was donated from Malaria Research and Reference Reagent Resource Center (MR4, Manassas, VA; deposited by CJ Janse and AP Waters, MR4 number: MRA-865). The infection was induced *via* intraperitoneal (*i.p.*) injection of 5×10^6 *P. berghei*-parasitized red blood cells (*Pb*RBCs) diluted in saline solution (200 μl), which were withdrawn from a previously infected mouse of the same strain. Uninfected animals received saline solution (200 μl, *i.p.*). LXA_4 treatment (0.5 μg/kg/day in 200 μl sterile saline) was performed by *i.p.* injection 2 h before infection. Untreated mice received the same volume of sterile saline. The treatment was performed daily, from day 1 to day 6 post-infection. Six days post-infection, a thick blood smear was performed for parasitemia determination using Diff-Quick staining. ECM was defined as the presentation of at least 2 of the following clinical signs of neurologic involvement: ataxia, limb paralysis, poor righting reflex, seizures, roll-over and coma. In addition, a set of 6 behavioral tests (transfer arousal, locomotor activity, tail elevation, wire maneuver, contact righting reflex, and righting in arena) adapted from the SHIRPA protocol [24,25] was used to provide a better estimate of the overall clinical status of the mice during infection. The performance in each test was assessed using the following scoring system: 0 to 5 (transfer arousal), 0 to 4 (locomotor activity), 0 to 4 (tail elevation), 0 to 4 (wire maneuver), 0 to 3 (contact righting reflex), and 0 to 3 (righting in arena). Tests were performed at day 0 and day 6 post-infection in 10 mice per group. The data are expressed as differences between the values registered at day 0 (pre-infection) and day 6 post-infection, from each individual mouse. Lower numbers represent maximum performance, whereas higher scores represent severe behavioral impairment. During all experimental of the procedures, the mice were monitored daily, and those that presented impaired locomotor activity and no struggle response to sequential handling were euthanized.

2.3. TNF-α determination from brain tissue

TNF-α levels were evaluated from brain tissue. Briefly, brains from non-infected, *P. berghei*-infected and LXA_4-treated *P. berghei*-infected mice were excised and homogenized in cell lysis buffer [20 mM TRIS, 150 mM NaCl, 5 mM KCl, 1% Triton X-100, protease inhibitor cocktail (1:1000, Sigma-Aldrich, USA)] and immediately frozen at −80 °C. The total protein content of each tissue homogenate was evaluated using the Bradford method, followed by determination of cytokine production using a standard sandwich ELISA, performed according to manufacturer's instructions (BD Pharmingen, USA). The plates were read at 490 nm in M5 Spectrophotometer (Molecular Devices, USA). The results were expressed as ng of cytokine per mg of tissue.

2.4. Evaluation of blood–brain barrier disruption

BBB disruption was evaluated as previously described [26]. The mice were infected and treated as described above. On day 5 post-infection, mice received an intravenous (*i.v.*) injection of 1% Evans blue dye (Sigma-Aldrich, Brazil) and were euthanized 1 h later. Their brains were weighed and placed in formamide (2 ml, 37 °C, 48 h) to extract the Evans blue dye from the brain tissue. Absorbance was measured at 620 nm (Spectramax 190, Molecular Devices, CA, USA). The concentration of Evans blue dye was calculated using a standard curve. The data are expressed as mg of Evans blue dye per g of brain tissue.

2.5. Cerebral intravital microscopy with epi-illumination and fluorescence

For intravital microscopy, the mice were infected and treated as described above. At day 5 post-infection, they were anesthetized *via i.p.* injection with a mixture of ketamine (100 mg/kg) and xylazine (10 mg/kg). Anesthesia was maintained *via* additional intravenous (*i.v.*) doses of 5 mg/kg *via* the tail vein. Core temperature was monitored with a rectal probe and was maintained at 37 °C with a homeothermic blanket (Harvard Apparatus, Boston, MA, USA).

To visualize the cerebral microcirculation, a craniotomy of the right parietal bone was performed using a drill to expose the *pia mater* microvasculature, as described previously [27]. This window also enables visualization of *in vivo* leukocyte recruitment [28]. The assessed field was continuously perfused with artificial cerebrospinal fluid at 37 °C, pH 7.35. The perfusate was continuously aerated with 10% O_2, 6% CO_2 and 84% N_2 to maintain tension and gas levels comparable to physiological pH and to avoid local inflammation.

Following *i.v.* administration of fluorescein dextran (FITC-dextran 150), images of the microcirculation were acquired using Archimed 3.7.0 software (Microvision, Evry, France). The capillary count was made using Saisam 5.1.3 software (Microvision). Serial images were taken with 10× ocular and 10× objective lenses (Olympus BX150WI; Center Valley, PA, USA) for 1 min/field from four fields. Only the continuously perfused capillaries were counted to determine the mean functional capillary density, expressed as the number of capillaries/mm^2.

To label circulating leukocytes, 0.3 mg/kg rhodamine 6G was *i.v.* injected. Fluorescing leukocytes were visualized *via* microscopy as described above. The leukocyte–endothelial interaction was evaluated by counting the number of leukocytes adhering to the venular wall (100 μm long) over 30 s and expressed as the number of cells/min/100 μm. Parameters were determined in *pia mater* venules with diameters ranging from 50 to 70 μm.

2.6. Brain histology

Brains from uninfected, *P. berghei*-infected and LXA_4-treated *P. berghei*-infected mice were carefully removed, fixed in 4% buffered formaldehyde, and paraffin-embedded. Five-micrometer-thick slices were cut and stained with hematoxylin and eosin. The cerebral microvasculature was analyzed in the cortical-medullary region. Occlusive vessels were examined in 30 consecutive fields under 400× magnification. Adhered parasitized red blood cells were assessed in 30 consecutive fields under 1000× magnification according to the following semi-quantitative scoring: 0 = no adhered parasitized red blood cells; 1 = unique adhered parasitized red blood cells; 2 = adhered rosettes; 3 = diffuse adhered cells.

2.7. Immunodetection of HO-1 and ICAM-1

Brains were removed from perfused mice and homogenized in ice-cold extraction buffer (50 mM Tris, pH 8.0, 150 mM NaCl, 1% NP-40) freshly supplemented with phosphatase and protease inhibitors (10 mM NaF, 5 mM Na_3VO_4, 5 mM $Na_4P_2O_7$ and 1× protease inhibitor cocktail, Sigma-Aldrich, USA). The final protein concentration in each condition was determined using the DC™ Protein assay reagent (Bio-Rad, USA), using BSA as a standard. Aliquots containing 30 μg of protein were re-suspended in SDS-PAGE loading buffer, resolved on 11% SDS acrylamide gels and transferred onto PVDF Hybond™ membranes (Amersham, UK). After blocking with 5% non-fat dry milk/Tris-buffered saline containing 0.1% Tween-20 for 1 h at room temperature, the membranes were probed overnight at 4 °C with specific primary antibodies followed by horseradish peroxidase-labeled secondary antibodies. Rabbit polyclonal anti-mouse HO-1 (1:5000) and horseradish peroxidase-labeled goat polyclonal anti-rabbit antibodies (1:2500) were obtained from Enzo Life Sciences, Inc. (USA). Mouse monoclonal anti-mouse ICAM-1 (1:1000) and horseradish peroxidase-labeled goat monoclonal anti-mouse antibodies (1:500) were obtained from Santa Cruz Biotechnologies, Inc. (USA). Then, PVDF sheets were incubated with streptavidin-conjugated horseradish peroxidase (1:10,000) for 1 h and developed by an ECL®-plus reagent (Enhanced Chemiluminescence, Amersham Biosciences). The bands were quantified by densitometry, using ImageJ (public domain) software programs.

The probed membranes were stripped with Re-Blot Plus Western Blot stripping solution (Millipore) for 30 min at room temperature and re-probed with rabbit polyclonal β-actin antibody to detect total levels of protein.

2.8. Endothelial cell stimulation

The murine thymic endothelioma cell line (tEnd.1) [29] and the human endothelial cell line ECV-304 [22] were kindly provided by Dr. T.C. Barja-Fidalgo (Universidade do Estado do Rio de Janeiro, Brazil). The endothelial cell lines ECV-304 or tEnd.1 were cultured in RPMI-1640 medium supplemented with 10% heat-inactivated FBS, 2 mM L-glutamine, 100 IU/ml penicillin and 100 mg/ml streptomycin. The cells were plated onto 24-well culture plates (Nunc, Rochester, NY, USA) and incubated (10^4 cells/well) at 37 °C in a humidified incubator containing 5% CO_2 chambers for 24 h. Before each experiment, ECV-304 or tEnd.1 cells were pretreated or not with LXA_4 (10 nM) for 1 h, the LXA_4 receptor antagonist BOC-2 (N-Boc-Phe-Leu-Phe-Leu-Phe, 40 nM) or the HO-1 inhibitor zinc protoporphyrin IX (ZnPPIX, 50 μM). *P. falciparum*-infected RBCs (*Pf*RBCs, kindly provided by Dr. M.G. Zalis, Universidade Federal do Rio de Janeiro) or *P. berghei*-infected RBCs (*Pb*RBCs) were stained with CFSE (25 μM; Life Technologies, USA) for 30 min and then added to both non-treated or treated the ECV-304 or tEnd.1 cultures (50 erythrocytes/cell, 5% parasitemia).

2.9. Cytoadherence assay

ECV-304 and tEnd.1 cells were cultured and treated as described above, and *Pf*RBCs or *Pb*RBCs were allowed to adhere to the ECV-304 or tEnd.1 cultures for 1 h. Non-adherent erythrocytes were gently washed away with PBS, and the remaining cells were subsequently fixed in ethanol and stained with Giemsa (Merck, Brazil). The number of adhered erythrocytes per ECV-304 or tEnd.1 cell was determined by direct counting under 400× magnification. The data are expressed as an association index calculated as previously described [30]: Adhesion index (AI) = (cell with bound erythrocytes) / total cell number × (erythrocytes bound to cell) / (total cell number × 100).

2.10. Immunocytochemistry

ECV-304 or tEnd.1 pre-treatment and stimulation were performed as described above. The immunofluorescent studies were performed as described previously [26]. To evaluate ICAM-1 expression, cells were fixed with 4% (w/v) paraformaldehyde and 4% (w/v) sucrose, followed by blocking with 2% bovine serum albumin. The cells were then incubated with anti-human ICAM-1 (1:50, BD Pharmingen, USA) mAb or anti-mouse ICAM-1 (1:100 BD Pharmingen, USA) and subsequently incubated with the appropriate secondary FITC-conjugated antibody (Santa Cruz Biotechnology, USA). Microscopic acquisition of the fluorescent images was performed using a fluorescence microscope (Nikon, Japan), and the fluorescence intensity was measured using Volocity software (Perkin Elmer, USA).

2.11. Statistical analysis

Statistical significance was assessed using ANOVA followed by the Bonferroni test. The results are expressed as the mean ± SEM, and the significance level in all cases was set at $p \leq 0.05$. A log-rank (Mantel–Cox) test was used to compare the percent survival. The significance level was set at $p \leq 0.05$.

3. Results

3.1. LXA_4 prevents cerebral dysfunction induced by *P. berghei* infection independently of TNF-α production

To address the involvement of LXA_4 on vascular dysfunction during ECM *P. berghei*-infected C57BL/6 mice were treated with LXA_4 (0.5 μg/kg/day). Initially, LXA_4 dose-response curves were constructed, and from these curves the threshold dose was defined (Supplemental data 1). LXA_4 treatment did not alter parasitemia levels 5 d post-infection (Fig. Fig. 1A), however, in agreement with a previous study [23], prolonged the survival of *P. berghei*-infected mice (Fig. Fig. 1B). Treatment with LXA_4 reduced the Evans blue dye extravasation into brain tissue observed during ECM (Fig. Fig. 1C). It is important to note that treatment with LXA_4 did not modulate Evans blue dye extravasation to the brain tissue of uninfected mice (Supplementary data 2). Moreover, LXA_4 treatment further improved behavioral and functional scores in treated mice compared with untreated mice (Fig. Fig. 1D). To investigate if LXA_4 ameliorates vascular dysfunction by modulating TNF-α production that accounts for activation of endothelial cells, we investigated TNF-α production in brain tissue of LXA_4 treated *P. berghei*-infected mice. A significant increase in TNF-α production was observed in the brains of *P. berghei* infected C57BL/6 mice compared to uninfected mice, however, the increased levels of TNF-α induced by *P. berghei* infection were not affected by LXA_4 treatment (Fig. Fig. 1E).

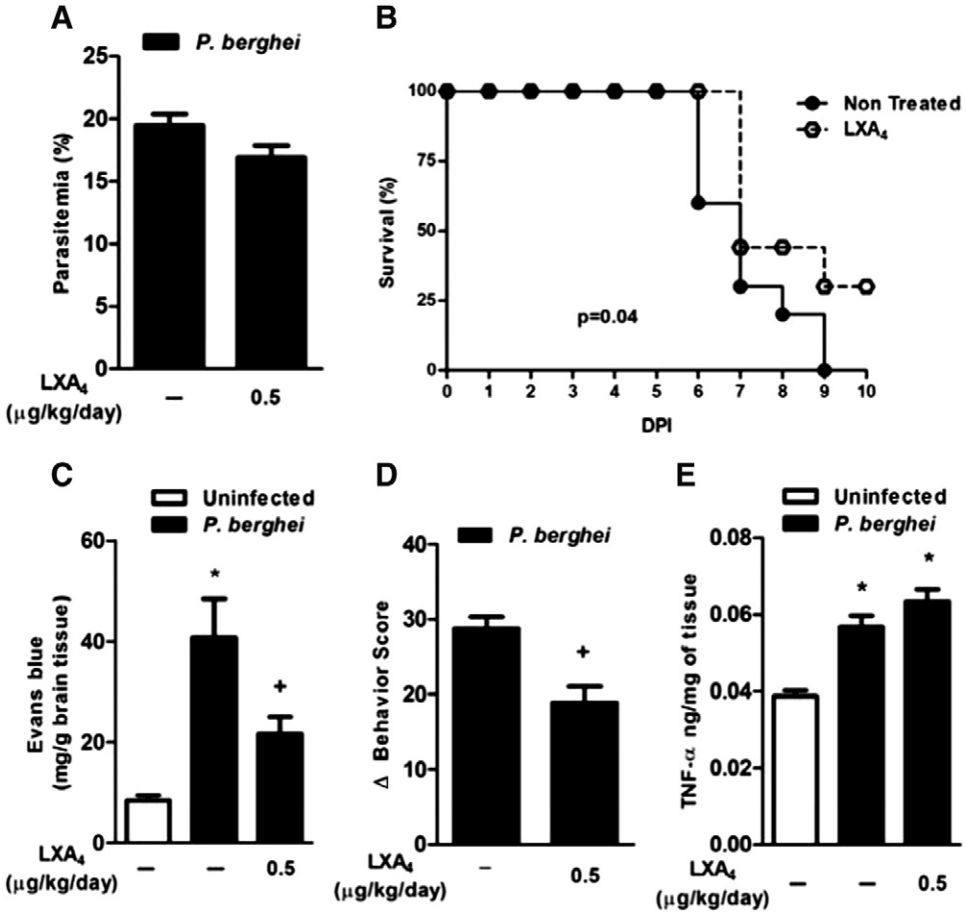

Fig. 1. LXA_4 attenuates cerebral malaria. (A) Parasitemia levels were evaluated 5 days post-infection in C57BL/6 infected with *P. berghei* and treated with LXA_4 (0.5 μg/kg/day), as described in Materials and methods. The results are expressed as the mean ± SEM from at least six animals per group in two independent experiments. (B) Survival rates for C57BL/6 mice infected with *P. berghei* untreated (vehicle, closed symbols) or treated with LXA_4 (0.5 μg/kg/day, open circle). The log-rank test revealed significantly different survival curves when untreated *P. berghei*-infected (n = 10) and LXA_4-treated *P. berghei*-infected (n = 10) C57BL/6 mice were compared (p = 0.04). (C) Evans blue dye extravasation within brain tissue from C57BL/6 mice uninfected (open bars) or *P. berghei*-infected (closed bars) 5 days prior. C57BL/6 mice were treated with LXA_4 (0.5 μg/kg/day). The results are expressed as the mean ± SEM from at least six animals per group in two independent experiments. (D) Behavioral and functional analyses were evaluated 5 days post-infection in C57BL/6 infected with *P. berghei* and treated with LXA_4 (0.5 μg/kg/day), as described in Materials and methods. The results of behavioral and functional analyses are expressed as differences between values registered pre- and post-infection (Δ) from at least six animals per group. (E) TNF-α levels from brain tissue were evaluated using ELISA. The results are expressed as the mean ± SEM of six animals per group. Statistically significant differences compared with the uninfected group ($p < 0.05$) are indicated by *, and statistically significant differences compared with the *P. berghei*-infected group ($p < 0.05$) are indicated by +.

3.2. LXA_4 ameliorates cerebral microcirculation of *P. berghei*-infected mice

Accordingly, a significant decrease in functional capillary density was observed due to diminished numbers of spontaneously perfused capillaries in the brains of *P. berghei*-infected mice (Fig. Fig. 2A and C) compared to uninfected mice (Fig. Fig. 2A and B). This phenomenon was partially reversed in LXA_4-treated mice (Fig. Fig. 2A and D). Accordingly, histological analyses of brain sections from infected mice treated with LXA_4 showed a reduction in the number of congested capillaries (Fig. Fig. 2E and H) compared to non-treated infected mice (Fig. Fig. 2E and G). In histological analyses of brain sections from uninfected mice it was not observed glial cell swelling neither capillary congestion (Fig. Fig. 2E and F). The diminished percentage of occluded vessels observed in LXA_4-treated mice was accompanied by lower score of parasitized erythrocytes adhesion to brain vasculature (Fig. Fig. 2I and L) then score observed in brain tissue of non-treated infected mice (Fig. Fig. 2I and K). No leukocytes were observed adhering to brain vasculature of non-infected mice (Fig. Fig. 2J).

3.3. LXA_4 inhibits endothelial activation markers during ECM

To investigate if the effects of LXA_4 are dependent of endothelial cell activation, the expression of endothelial activation marker ICAM-1 was quantified in brain tissue of *P. berghei* infected mice, treated or not treated with LXA_4. As expected, ICAM-1 expression was higher in *P. berghei* infected mice than in uninfected mice, and LXA_4 treatment reduced ICAM-1 expression in the brains of *P. berghei*-infected mice (Fig. Fig. 3A). Corroborating such results, the co-culture of murine endothelial cells (tEnd.1 cells) and red blood cells parasitized by *P. berghei* (*Pb*RBCs) induced the expression of ICAM-1 expression (Fig. Fig. 3B). In agreement, *P. falciparum*-infected red blood cells (*Pf*RBCs) also induced ICAM-1 expression in human endothelial cells (ECV-304 cells) (Fig. Fig. 3C). Interestingly, the treatment of both endothelial cell lines with LXA_4 impaired ICAM-1 expression when compared with the equivalent parasitized RBC-stimulated control group. Treatment with BOC-2 reversed the decreased ICAM-1 expression induced by LXA_4 (Fig. Fig. 3B and C).

3.4. LXA_4 triggers cytoprotective pathways during ECM

To address the hypothesis that LXA_4 triggers endothelial protective effects during ECM, we evaluated a mechanism by which LXA_4 ameliorates endothelial cell function in *P. berghei*-infected mice. To this end, the expression of HO-1 was quantified in brain tissue of *P. berghei* infected mice, treated or not treated with LXA_4. Low levels of HO-1 were detected in the brains of *P. berghei* infected mice when compared with

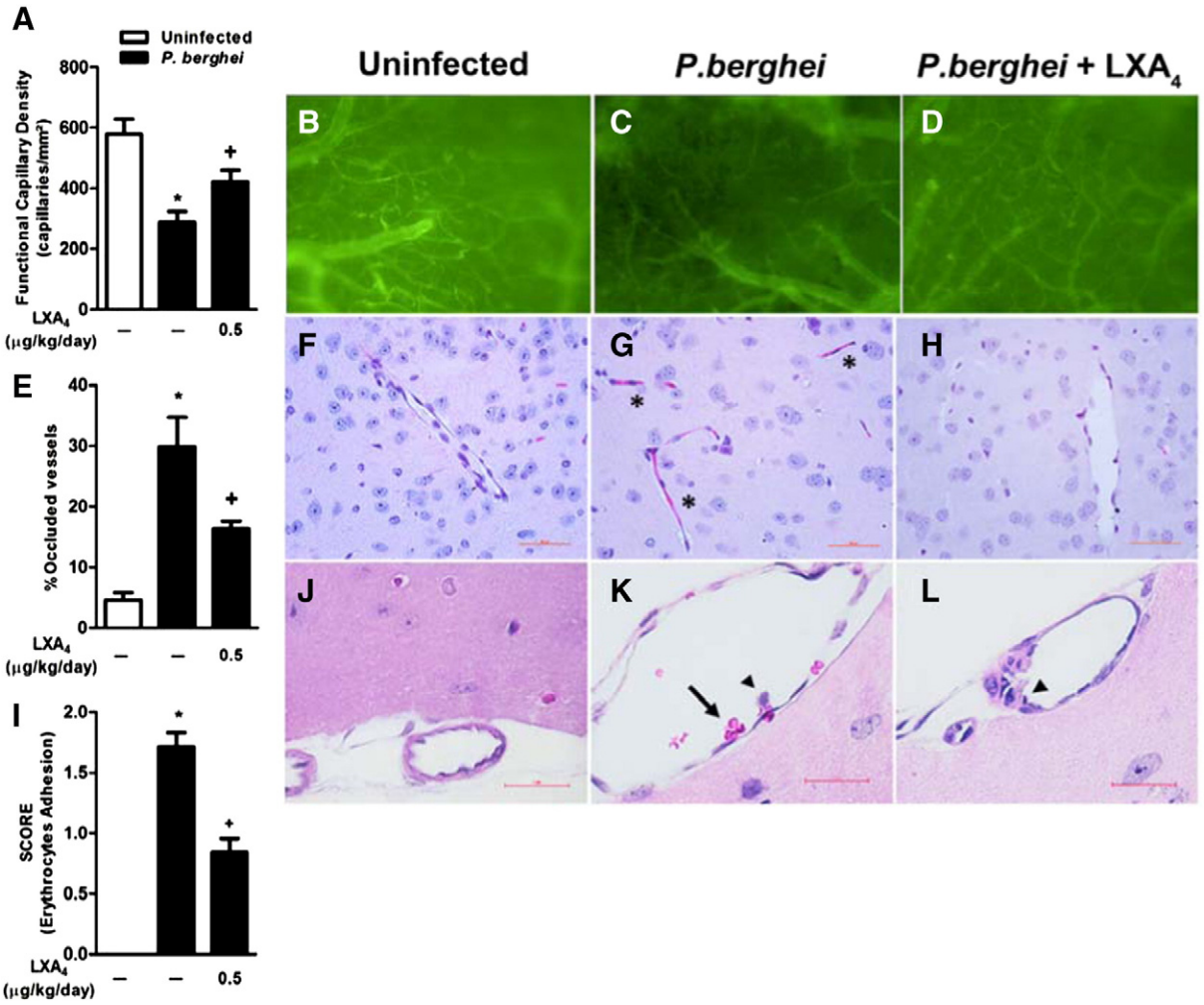

Fig. 2. LXA_4 effects on brain vascular dysfunction during *P. berghei* infection. (A) Intravital microscopy was performed on brains from C57BL/6 mice either uninfected (open bars) or infected with *P. berghei* (closed bars) 5 days prior and functional capillary density were analyzed. Representative images of pial vessels in uninfected mice (B), *P. berghei*-infected mice (C) and *P. berghei*-infected and LXA_4-treated (0.5 μg/kg/day; D). (E) The percentage of occluded vessels in brain sections recovered from uninfected (open bars), *P. berghei*-infected (closed bars) and *P. berghei*-infected and LXA_4-treated (0.5 μg/kg/day) C57BL/6 mice. (I) Semi-quantitative analysis of cell adhesion in brain vessels. Values are expressed as the mean of 30 consecutive fields per slide from 6 animals in each group, and the score of erythrocyte adhesion was defined as described in the Materials and methods section. The results are expressed as the mean ± SEM from at least six animals per group in two independent experiments. Statistically significant differences compared with the uninfected group ($p < 0.05$) are indicated by *, and statistically significant differences compared with the *P. berghei*-infected group ($p < 0.05$) are indicated by +. Representative photomicrographs of brains from uninfected mice (F and J), *P. berghei*-infected mice (G and K) and *P. berghei*-infected and LXA_4-treated (0.5 μg/kg/day; H and L) demonstrating occluded vessels (*), RBCs adhered to the endothelium (black arrows) and leukocytes adhered to the endothelium (head arrows).

uninfected mice; and LXA_4-treated mice expressed similarly elevated levels of HO-1 over those observed in uninfected mice (Fig. Fig. 4A). Additionally, the co-culture of endothelial cells and parasitized red blood cells (either *Pb*RBCs or *Pf*RBCs) induced the adhesion of parasitized RBCs to the membranes of the respective endothelial cells. Adhesion was inhibited when both cell lines were pretreated with LXA_4 (10 nM) and treatment with BOC-2 (40 nM) reversed the inhibitory effect of LXA_4. To evaluate the mechanism by which LXA_4 modulates parasitized RBC adhesion to endothelial cells, the cells were further treated with ZnPPIX (50 μM) to block the activity of HO-1. We observed that LXA_4-reduced RBC adhesion was reversed by ZnPPIX pretreatment of both endothelial cell lines (Fig. Fig. 4B and C, Supplementary data 2).

4. Discussion

Herein, using an experimental model of cerebral malaria, we demonstrate for the first time that LXA_4 exerts an endothelial protective effect during ECM by inducing cytoprotective pathways. Despite its widely recognized role as anti-inflammatory mediator [13,19,31,32], the role of LXA_4 during cerebral dysfunction induced by malaria infection is poorly understood.

Previous data in the literature have shown that treatment with the LXA_4 epimer improved mouse survival by inhibiting IL-12 production and $CD8^+IFN\text{-}\gamma^+$ T cell accumulation in brain tissue [23]. In agreement with these results, we observed amelioration of major signs of ECM as cerebral edema and behavioral and functional scores. Interestingly, when we performed a dose–response experiment aimed to pharmacologically investigate the link between LXA_4 levels and its effects, we observed that lower doses were more effective. As described before, the LXA_4 receptor, ALX/FPRL, is a G-protein coupled receptor (GPCR) involved in cell- and agonist-specific signaling [33]. Furthermore, ALX/FRPL is regulated by desensitization and agonist-induced internalization [34]. Thus, in our model, where LXA_4 is administered for 6 days, higher doses of LXA_4 are most likely inducing internalization and/or desensitization. In addition, LXA_4 did not interfere with parasitemia levels, supporting the evidence that LXA_4 modulates exclusively the host response to *P. berghei* infection.

Cerebral tissue damage induced during *P. berghei* infection is primarily due to inflammatory cell accumulation/activation, the production of

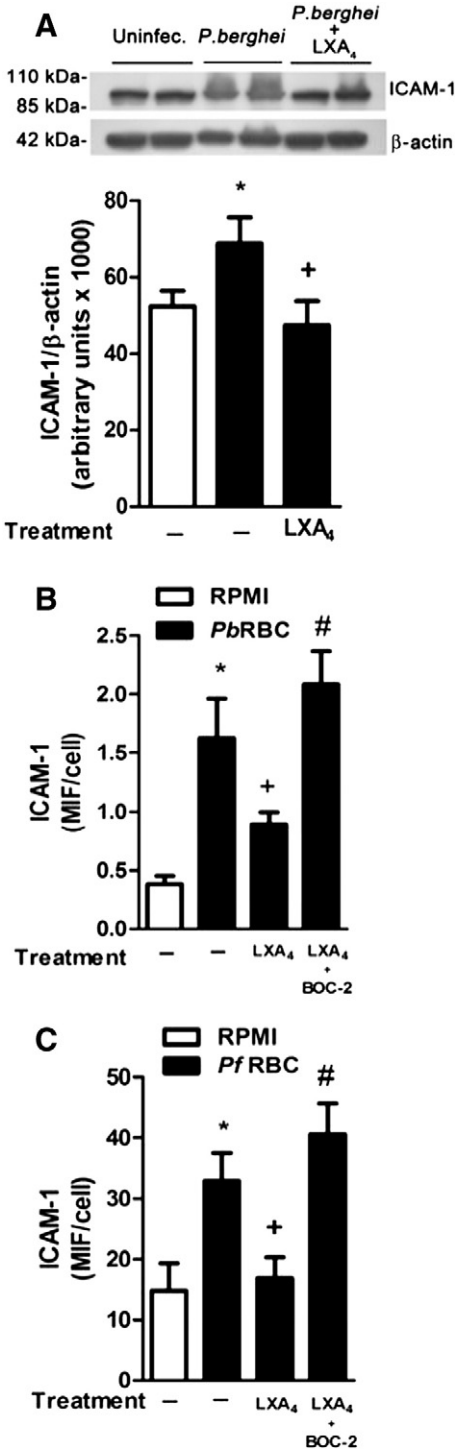

Fig. 3. LXA_4 inhibit ICAM-1 expression during *P. berghei* infection *in vivo* and *in vitro*. (A) Representative membrane preparations of uninfected (lanes 1 and 2, open bars), *P. berghei*-infected (lanes 3 and 4, closed bars) and *P. berghei*-infected and LXA_4-treated (0.5 μg/kg/day; lanes 5 and 6) underwent immunoblotting for the detection of ICAM-1 in brain tissue. ICAM-1 expression levels were normalized to β-actin. The results are expressed as the means ± SEM (n = 6) of two independent experiments. Statistically significant differences compared with the uninfected group ($p < 0.05$) are indicated by *, and statistically significant differences compared with the *P. berghei*-infected group ($p < 0.05$) are indicated by +. The murine tEnd.1 endothelial cell line (B) and human ECV-304 endothelial cell line (C) were used to determine ICAM-1 expression under parasitized RBC stimulation. ICAM-1 expression levels were evaluated in endothelial cells pretreated with LXA_4 (10 nM) or LXA_4 plus BOC-2 (40 nM) and stimulated with parasitized (*P. berghei* — *Pb*; *P. falciparum* — *Pf*) RBCs. The results are expressed as the MIF ± SEM from three independent experiments. Statistically significant differences compared with the parasitized RBC untreated group ($p < 0.05$) are indicated by +, significant differences compared with the LXA_4 treated group are indicated by #, and significant differences between unstimulated and parasitized RBC-stimulated cells are indicated by *.

inflammatory mediators in the brain vasculature, and the breakdown of the BBB. This latter effect is induced by decreased expression of junction proteins in activated cerebral endothelial cells [3,35,36]. Lipoxins have been described to ameliorate BBB breakdown in non-infectious experimental models by modulating MMP9 expression and MAPK activation [37,38]. Compelling evidence suggests that the protective role of LXA_4 in diseases caused by apicomplexan parasites such as *Toxoplasma gondii* [39,40] depends on inhibition of cytokine production. Accordingly, increased production of IFN-γ and IL-12 has been demonstrated during ECM in the absence of endogenous LXA_4 [23]. It is noteworthy that IFN-γ and IL-12 are more relevant in lymphocyte activation rather than endothelial activation [41]. TNF-α has been demonstrated as a crucial cytokine in endothelial dysfunction during ECM [42,43]. However, in our model, LXA_4 did not modulate TNF-α production during ECM. As well, LXA_4 impairs the activation of TNF-α-stimulated endothelial cells [22,44], which suggests that prevention of brain edema formation in LXA_4-treated mice does not depend on TNF-α production. Although the modulation of cytokines by LXA_4 treatment during severe malaria cannot be excluded, our results concerning cerebral dysfunction strongly suggested an additional role to the many played by this lipid mediator in ECM.

Although we did not observe a difference in lymphocyte accumulation in the brain tissue of LXA_4-infected mice (data not shown), we observed an improved functional capillary density, a significant reduction in vascular occlusion in the brains of LXA_4-treated mice and reduced *P. berghei*-infected erythrocytes adhered to brain vasculature. Indeed, ECM is associated with vasoconstriction and impaired responses to acetylcholine due to nitric oxide synthase dysfunction [45,46]. Thus, therapeutic approaches for improving endothelial function, such as the induction of HO-1 expression and reduction of ICAM-expression through the administration of either NO donors [47] or carbon monoxide [12], would be beneficial in *P. berghei* infection.

To confirm the hypothesis that LXA_4 is acting on endothelial dysfunction induced during ECM, the expression of endothelial cell activation marker, ICAM-1, was investigated. In the current study, LXA_4 impaired ICAM-1 expression in brain tissue of infected mice, as well as in *Pb*RBCs- and *Pf*RBCs-stimulated endothelial cells *in vitro*. The ability of the LXA_4/ALX complex to modulate the expression of adhesion molecules has been described in other non-infectious models, including their capability to reduce the expression of ICAM-1 on TNF-α-stimulated endothelial cells *in vitro* [48,49]. Under inflammatory conditions, ICAM-1 signaling is involved in endothelial activation, the rearrangement of the endothelial actin cytoskeleton, the regulation of vascular permeability, and the transmigration of immune cells into the brain parenchyma [50,51]. The essential role of ICAM-1 in cytoadherence and vascular occlusion during ECM has been previously demonstrated [26]; however, until now, the direct effect of LXA_4 on the inhibition of ICAM-1 expression during ECM had not been shown.

Several studies have described that LXA_4-induced HO-1 expression attenuates endothelial dysfunction both *in vivo* [52,53] and *in vitro* [22,54]. HO-1 is an isoenzyme that catabolizes free heme released under pathological conditions, especially in pathologies that are associated with intravascular hemolysis, such as burns, microangiopathy and malaria. HO-1 expression is related to tissue protection [21]. Indeed, the presence of HO-1 limits the damage induced during the inflammatory response, and its pharmacological up-regulation helps maintain BBB integrity under pathological conditions *in vivo* and *in vitro* [55]. It has been widely described that HO-1 inhibits the expression of several adhesion molecules, especially ICAM-1 [56,57]. As well, the modulation of adhesion molecules by LXA_4 *via* HO-1 expression in TNF-α-stimulated cells has already been demonstrated [22]. In addition, parasites export protein to erythrocyte membrane that allows parasitized red blood cell adhesion to adhesion molecules expressed on endothelial cells [42,58]. During ECM, HO-1 is known to be differentially regulated in certain tissues at different stages of the *Plasmodium* life cycle [12,59]. Furthermore, HO-1 production in brain tissue is associated with mouse survival,

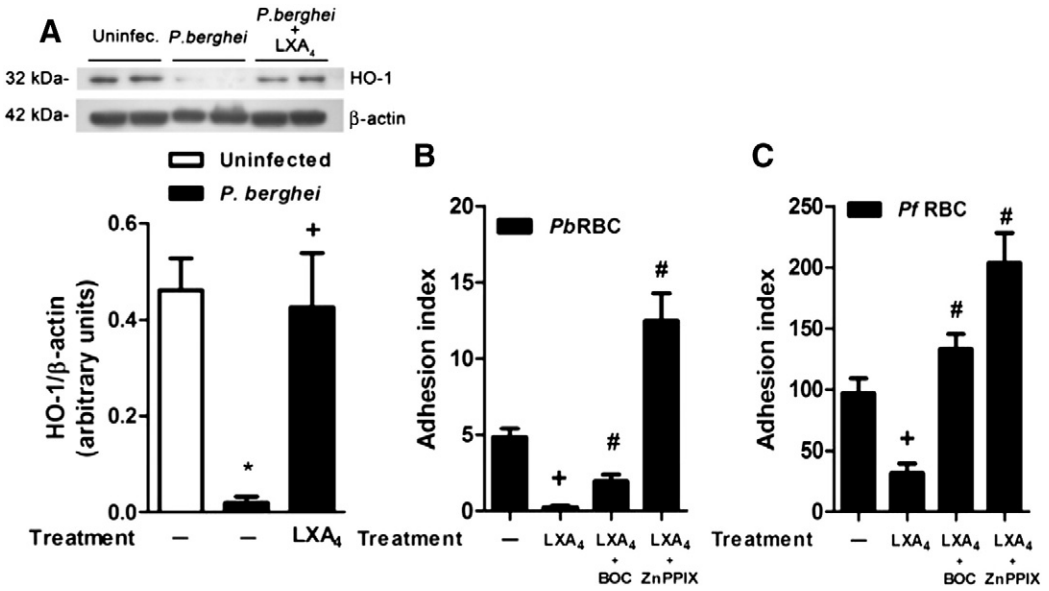

Fig. 4. LXA_4-induced HO-1 attenuates endothelial dysfunction induced by parasitized RBCs. (A) Representative membrane preparations of uninfected (lanes 1 and 2, open bars), *P. berghei*-infected (lanes 3 and 4, closed bars) and *P. berghei*-infected and LXA_4-treated (0.5 μg/kg/day; lanes 5 and 6) underwent immunoblotting for the detection of HO-1 in brain tissue. HO-1 expression levels were normalized to β-actin. The results are expressed as the means ± SEM (n = 6) of two independent experiments. Statistically significant differences compared with the uninfected group ($p < 0.05$) are indicated by *, and statistically significant differences compared with the *P. berghei*-infected group ($p < 0.05$) are indicated by +. The adhesion of *Pb*RBCs (B) to tEnd.1 or *Pf*RBCs (C) to ECV-304 was calculated using the adhesion index as described in the Materials and methods section. Adhesion index was evaluated in endothelial cells lines pretreated with LXA_4 (10 nM), LXA_4 plus BOC-2 (40 nM) and LXA_4 plus ZnPPIX (50 μM) and stimulated with parasitized RBCs. The results are expressed as the mean ± SEM from three independent experiments. Statistically significant differences compared with the parasitized RBC untreated group ($p < 0.05$) are indicated by +, significant differences compared with the LXA_4 treated group are indicated by #.

decreased cerebral edema and decreased ICAM-1 expression [12]. However, even though LXA_4 has been demonstrated to induce HO-1 expression in non-infectious models *in vivo* [60], this effect has not been previously demonstrated in a malaria model. Thus, in our model, LXA_4 probably reduces the ICAM-1 expression by inducing the expression of HO-1.

Collectively, the results of this study suggest that LXA_4 attenuates cerebral dysfunction by regulating the expression of ICAM-1 and HO-1 both *in vivo* and *in vitro*.

5. Author's contributions

MCS and TAP designed and performed experiments, analyzed data and wrote the paper. NDT performed experiments and analyzed data. MFSC, APC, TM, LNS, VE, BA, LS performed experiments and analyzed data. ACA, CCN, and ET designed and supervised experiments. LC designed experiments and assisted in drafting this manuscript. MCS and MGH conceived the study, designed and supervised experiments and assisted in drafting this manuscript. All authors read and approved the final manuscript.

Acknowledgments

The authors would like to express their gratitude to Dr. Octávio Menezes de Lima Junior at the Laboratory of Applied Pharmacology (Farmanguinhos, FIOCRUZ) for his critical reading of this manuscript. This work was supported by grants from the Brazilian Council for Scientific and Technological Development (CNPq: 481286/2013-6, 304588/2010-5 and 475262/2013), the Rio de Janeiro State Research Supporting Foundation Carlos Chagas Filho (FAPERJ: E-26/102335/2013, E-36/110605/2012, E-26/111.724/2013 and 111.272/2014), the Coordination for the Improvement of Higher Education Personnel (CAPES: 149/2007), and Fundação Oswaldo Cruz (FIOCRUZ: 407766/2012).

Appendix A. Supplementary data

Supplementary data to this article can be found online at http://dx.doi.org/10.1016/j.intimp.2014.12.033.

References

[1] Murray CJ, Rosenfeld LC, Lim SS, Andrews KG, Foreman KJ, Haring D, et al. Global malaria mortality between 1980 and 2010: a systematic analysis. Lancet 2012;379:413–31.
[2] Medana IM, Turner GD. Human cerebral malaria and the blood–brain barrier. Int J Parasitol 2006;36:555–68.
[3] Nacer A, Movila A, Baer K, Mikolajczak SA, Kappe SHI, Frevert U. Neuroimmunological blood brain barrier opening in experimental cerebral malaria. PLoS Pathog 2012;8.
[4] Baptista FG, Pamplona A, Pena AC, Mota MM, Pied S, Vigario AM. Accumulation of *Plasmodium berghei*-infected red blood cells in the brain is crucial for the development of cerebral malaria in mice. Infect Immun 2010;78:4033–9.
[5] Amante FH, Haque A, Stanley AC, Rivera Fde L, Randall LM, Wilson YA, et al. Immune-mediated mechanisms of parasite tissue sequestration during experimental. J Immunol 2010;185:3632–42.
[6] McQuillan JA, Mitchell AJ, Ho YF, Combes V, Ball HJ, Golenser J, et al. Coincident parasite and CD8 T cell sequestration is required for development of experimental cerebral malaria. Int J Parasitol 2011;41:155–63.
[7] Souza MC, Silva JD, Padua TA, Capelozzi VL, Rocco PRM, MdG Henriques. Early and late acute lung injury and their association with distal organ damage in murine malaria. Respir Physiol Neurobiol 2013;186:65–72.
[8] Haque A, Best SE, Unosson K, Amante FH, de Labastida F, Anstey NM, et al. Granzyme B expression by CD8+ T cells is required for the development of experimental cerebral malaria. J Immunol 2011;186:6148–56.
[9] Bergmark B, Bergmark R, Beaudrap PD, Boum Y, Mwanga-Amumpaire J, Carroll R, et al. Inhaled nitric oxide and cerebral malaria: basis of a strategy for buying time for pharmacotherapy. Pediatr Infect Dis J 2012;31:e250–4.
[10] Carvalho LJ, Moreira AD, Daniel-Ribeiro CT, Martins YC. Vascular dysfunction as a target for adjuvant therapy in cerebral malaria. Mem Inst Oswaldo Cruz 2014;109:577–88.
[11] Kim H, Higgins S, Liles WC, Kain KC. Endothelial activation and dysregulation in malaria: a potential target for novel therapeutics. Curr Opin Hematol 2011;18:177–85.
[12] Pamplona A, Ferreira A, Balla J, Jeney V, Balla G, Epiphanio S, et al. Heme oxygenase-1 and carbon monoxide suppress the pathogenesis of experimental cerebral malaria. Nat Med 2007;13:703–10.
[13] Ryan A, Godson C. Lipoxins: regulators of resolution. Curr Opin Pharmacol 2010;10:166–72.

[14] Haworth O, Cernadas M, Yang R, Serhan CN, Levy BD. Resolvin E1 regulates interleukin 23, interferon-gamma and lipoxin A4 to promote the resolution of allergic airway inflammation. Nat Immunol 2008;9:873–9.
[15] Chan MM, Moore AR. Resolution of inflammation in murine autoimmune arthritis is disrupted by cyclooxygenase-2 inhibition and restored by prostaglandin E2-mediated lipoxin A4 production. J Immunol 2010;184:6418–26.
[16] Chen M, Divangahi M, Gan H, Shin DS, Hong S, Lee DM, et al. Lipid mediators in innate immunity against tuberculosis: opposing roles of PGE2 and LXA4 in the induction of macrophage death. J Exp Med 2008;205:2791–801.
[17] Nascimento-Silva V, Arruda MA, Barja-Fidalgo C, Fierro IM. Aspirin-triggered lipoxin A4 blocks reactive oxygen species generation in endothelial cells: a novel antioxidative mechanism. Thromb Haemost 2007;97:88–98.
[18] Cezar-de-Mello PF, Vieira AM, Nascimento-Silva V, Villela CG, Barja-Fidalgo C, Fierro IM. ATL-1, an analogue of aspirin-triggered lipoxin A4, is a potent inhibitor of several steps in angiogenesis induced by vascular endothelial growth factor. Br J Pharmacol 2008;153:956–65.
[19] Wu SH, Liao PY, Dong L, Chen ZQ. Signal pathway involved in inhibition by lipoxin A(4) of production of interleukins induced in endothelial cells by lipopolysaccharide. Inflamm Res 2008;57:430–7.
[20] Fiorucci S, Distrutti E, Mencarelli A, Morelli A, Laufor SA, Cirino G, et al. Evidence that 5-lipoxygenase and acetylated cyclooxygenase 2-derived eicosanoids regulate leukocyte-endothelial adherence in response to aspirin. Br J Pharmacol 2003;139:1351–9.
[21] Gozzelino R, Jeney V, Soares MP. Mechanisms of cell protection by heme oxygenase-1. Annu Rev Pharmacol Toxicol 2010;50:323–54.
[22] Nascimento-Silva V, Arruda MA, Barja-Fidalgo C, Villela CG, Fierro IM. Novel lipid mediator aspirin-triggered lipoxin A4 induces heme oxygenase-1 in endothelial cells. Am J Physiol Cell Physiol 2005;289:C557–63.
[23] Shryock N, McBerry C, Salazar Gonzalez RM, Janes S, Costa FT, Aliberti J. Lipoxin A(4) and 15-epi-lipoxin A(4) protect against experimental cerebral malaria by inhibiting IL-12/IFN-gamma in the brain. PLoS One 2013;8:e61882.
[24] Martins YC, Werneck GL, Carvalho LJ, Silva BP, Andrade BG, Souza TM, et al. Algorithms to predict cerebral malaria in murine models using the SHIRPA protocol. Malar J 2010;9:85.
[25] Lackner P, Beer R, Heussler V, Goebel G, Rudzki D, Helbok R, et al. Behavioural and histopathological alterations in mice with cerebral malaria. Neuropathol Appl Neurobiol 2006;32:177–88.
[26] Souza MC, Paixao FH, Ferraris FK, Ribeiro I, Henriques M. Artesunate exerts a direct effect on endothelial cell activation and NF-kappaB translocation in a mechanism independent of *Plasmodium* killing. Malar Res Treat 2012;2012:679090.
[27] Araújo CV, Estato V, Tibirica E, Bozza PT, Castro-Faria-Neto HC, Silva AR. PPAR gamma activation protects the brain against microvascular dysfunction in sepsis. Microvasc Res 2012;84:218–21.
[28] Carvalho-Tavares J, Hickey MJ, Hutchison J, Michaud J, Sutcliffe IT, Kubes P. A role for platelets and endothelial selectins in tumor necrosis factor-alpha-induced leukocyte recruitment in the brain microvasculature. Circ Res 2000;87:1141–8.
[29] Ferraris FK, Rodrigues R, da Silva VP, Figueiredo R, Penido C, Henriques M. Modulation of T lymphocyte and eosinophil functions in vitro by natural tetranortriterpenoids isolated from *Carapa guianensis* Aublet. Int Immunopharmacol 2011;11:1–11.
[30] Roffe E, Silva AA, Marino AP, dos Santos PV, Lannes-Vieira J. Essential role of VLA-4/VCAM-1 pathway in the establishment of CD8+ T-cell-mediated *Trypanosoma cruzi*-elicited meningoencephalitis. J Neuroimmunol 2003;142:17–30.
[31] Menezes-de-Lima Jr O, Kassuya CA, Nascimento AF, Henriques M, Calixto JB. Lipoxin A4 inhibits acute edema in mice: implications for the anti-edematogenic mechanism induced by aspirin. Prostaglandins Other Lipid Mediat 2006;80:123–35.
[32] Pang H, Yi P, Wu P, Liu Z, Gong J, Hao H, et al. Effect of lipoxin A4 on lipopolysaccharide-induced endothelial hyperpermeability. Sci World J 2011;11:1056–67.
[33] Romano M, Recchia I, Recchiuti A. Lipoxin receptors. Sci World J 2007;7:1393–412.
[34] Le Y, Oppenheim JJ, Wang JM. Pleiotropic roles of formyl peptide receptors. Cytokine Growth Factor Rev 2001;12:91–105.
[35] Pino P, Taoufiq Z, Nitcheu J, Vouldoukis I, Mazier D. Blood–brain barrier breakdown during cerebral malaria: suicide or murder? Thromb Haemost 2005;94:336–40.
[36] de Souza JB, Hafalla JC, Riley EM, Couper KN. Cerebral malaria: why experimental murine models are required to understand the pathogenesis of disease. Parasitology 2010;137:755–72.
[37] Wu Y, Wang YP, Guo P, Ye XH, Wang J, Yuan SY, et al. A lipoxin A4 analog ameliorates blood–brain barrier dysfunction and reduces MMP-9 expression in a rat model of focal cerebral ischemia–reperfusion injury. J Mol Neurosci 2012;46:483–91.
[38] Luo CL, Li QQ, Chen XP, Zhang XM, Li LL, Li BX, et al. Lipoxin A4 attenuates brain damage and downregulates the production of pro-inflammatory cytokines and phosphorylated mitogen-activated protein kinases in a mouse model of traumatic brain injury. Brain Res 2013;1502:1–10.
[39] Aliberti J, Hieny S, Reise Sousa C, Serhan CN, Sher A. Lipoxin-mediated inhibition of IL-12 production by DCs: a mechanism for regulation of microbial immunity. Nat Immunol 2002;3:76–82.
[40] Aliberti J, Serhan C, Sher A. Parasite-induced lipoxin A4 is an endogenous regulator of IL-12 production and immunopathology in *Toxoplasma gondii* infection. J Exp Med 2002;196:1253–62.
[41] Villegas-Mendez A, Greig R, Shaw TN, de Souza JB, Findlay EG, Stumhofer JS, et al. IFN-γ producing CD4+ T cells promote experimental cerebral malaria by modulating CD8+ T cell accumulation within the brain. J Immunol 2012;189:968–79.
[42] El-Assaad F, Wheway J, Mitchell AJ, Lou J, Hunt NH, Combes V, et al. Cytoadherence of *Plasmodium berghei*-infected red blood cells to murine brain and lung microvascular endothelial cells in vitro. Infect Immun 2013;81:3984–91.
[43] Togbe D, de Sousa PL, Fauconnier M, Boissay V, Fick L, Scheu S, et al. Both functional LTbeta receptor and TNF receptor 2 are required for the development of experimental cerebral malaria. PLoS One 2008;3:e2608.
[44] Liao BC, Hsieh CW, Liu YC, Tzeng TT, Sun YW, Wung BS. Cinnamaldehyde inhibits the tumor necrosis factor-alpha-induced expression of cell adhesion molecules in endothelial cells by suppressing NF-kappaB activation: effects upon IkappaB and Nrf2. Toxicol Appl Pharmacol 2008;229:161–71.
[45] Ong PK, Melchior B, Martins YC, Hofer A, Orjuela-Sanchez P, Cabrales P, et al. Nitric oxide synthase dysfunction contributes to impaired cerebroarteriolar reactivity in experimental cerebral malaria. PLoS Pathog 2013;9:e1003444.
[46] Cabrales P, Zanini GM, Meays D, Frangos JA, Carvalho LJ. Murine cerebral malaria is associated with a vasospasm-like microcirculatory dysfunction, and survival upon rescue treatment is markedly increased by nimodipine. Am J Pathol 2010;176:1306–15.
[47] Orjuela-Sanchez P, Ong PK, Zanini GM, Melchior B, Martins YC, Meays D, et al. Transdermal glyceryl trinitrate as an effective adjunctive treatment with artemether for late-stage experimental cerebral malaria. Antimicrob Agents Chemother 2013;57:5462–71.
[48] Merched AJ, Serhan CN, Chan L. Nutrigenetic disruption of inflammation-resolution homeostasis and atherogenesis. J Nutrigenet Nutrigenomics 2011;4:12–24.
[49] Chinthamani S, Odusanwo O, Mondal N, Nelson J, Neelamegham S, Baker OJ. Lipoxin A4 inhibits immune cell binding to salivary epithelium and vascular endothelium. Am J Physiol Cell Physiol 2012;302:C968–78.
[50] Etienne-Manneville S, Manneville JB, Adamson P, Wilbourn B, Greenwood J, Couraud PO. ICAM-1-coupled cytoskeletal rearrangements and transendothelial lymphocyte migration involve intracellular calcium signaling in brain endothelial cell lines. J Immunol 2000;165:3375–83.
[51] Dietrich JB. The adhesion molecule ICAM-1 and its regulation in relation with the blood–brain barrier. J Neuroimmunol 2002;128:58–68.
[52] Jin SW, Zhang L, Lian QQ, Liu D, Wu P, Yao SL, et al. Posttreatment with aspirin-triggered lipoxin A4 analog attenuates lipopolysaccharide-induced acute lung injury in mice: the role of heme oxygenase-1. Anesth Analg 2007;104:369–77.
[53] Wang YZ, Zhang YC, Cheng JS, Ni Q, Li PJ, Wang SW, et al. BML-111, a lipoxin receptor agonist, ameliorates 'two-hit'-induced acute pancreatitis-associated lung injury in mice by the upregulation of heme oxygenase-1. Artif Cells Nanomed Biotechnol 2014;42:110–20.
[54] Lv W, Lv C, Yu S, Yang Y, Kong H, Xie J, et al. Lipoxin A4 attenuation of endothelial inflammation response mimicking pancreatitis-induced lung injury. Exp Biol Med (Maywood) 2013;238:1388–95.
[55] Wang YF, Gu YT, Qin GH, Zhong L, Meng YN. Curcumin ameliorates the permeability of the blood–brain barrier during hypoxia by upregulating heme oxygenase-1 expression in brain microvascular endothelial cells. J Mol Neurosci 2013;51:344–51.
[56] Lu CY, Yang YC, Li CC, Liu KL, Lii CK, Chen HW. Andrographolide inhibits TNFalpha-induced ICAM-1 expression via suppression of NADPH oxidase activation and induction of HO-1 and GCLM expression through the PI3K/Akt/Nrf2 and PI3K/Akt/AP-1 pathways in human endothelial cells. Biochem Pharmacol 2014;91:40–50.
[57] Belhaj A, Dewachter L, Kerbaul F, Brimioulle S, Dewachter C, Naeije R, et al. Heme oxygenase-1 and inflammation in experimental right ventricular failure on prolonged overcirculation-induced pulmonary hypertension. PLoS One 2013;8:e69470.
[58] Gullingsrud J, Saveria T, Amos E, Duffy PE, Oleinikov AV. Structure–function–immunogenicity studies of PfEMP1 domain DBL2betaPF11_0521, a malaria parasite ligand for ICAM-1. PLoS One 2013;8:e61323.
[59] Seixas E, Gozzelino R, Chora A, Ferreira A, Silva G, Larsen R, et al. Heme oxygenase-1 affords protection against noncerebral forms of severe malaria. Proc Natl Acad Sci U S A 2009;106:15837–42.
[60] Wu L, Liu ZJ, Miao S, Zou LB, Cai L, Wu P, et al. Lipoxin A4 ameliorates cerebral ischaemia/reperfusion injury through upregulation of nuclear factor erythroid 2-related factor 2. Neurol Res 2013;35:968–75.